IJISET - International Journal of Innovative Science, Engineering & Technology, Vol. 13 Issue 07, July 2026
ISSN (Online) 2348 – 7968 | Impact Factor – 6.72
www.ijiset.com

Determination of Optical Properties of Carbon Nanotubes Doped with Aluminum oxide Nanomaterial's for Different Molars Concentrations Using Ultraviolet-Visible Spectroscopy, X-Ray Diffraction and Infrared Techniques

Hasabalrasoul. G. Ismail[1], Amal Mohammed Abass M[o]hammed[1], Sana Ali Ahmed Mohamed[1], Nagi AbdAlla Ali AbdAlla[2], B.A.B Alawad[3], Mubarak Dirar AbdAlla[3], A. H. Abdelrahman[4]

[1] Department of Physics & Mathematics, Faculty of Education –El-Hasaheisa, Gezira University, Wad Madani, Sudan.
hasabo251@uofg.edu,sd, hasabo251@gmail.com
2 Department of Physics, Faculty of Education, University of Dongla, Dongla, Sudan
3 Department of Physics, Faculty of Science, Sudan University of Science and Technology, Khartoum, Sudan
[4]Department of Physics, College of Science, Qassim University, 51452 Buraidah, Saudi Arabia, a.yassin@qu.edu.sa

Abstract

The aim of this study is the determination of the optical properties of carbon nanotubes doped with Aluminum oxide nanomaterial for different molar concentrations (0.1, 0.3, 0.5, 0.7 and 0.9). The techniques used for studying optical properties are ultraviolet and infrared techniques. For nanoscale samples, the X-ray diffraction technique was used. The results of the study of optical properties using the ultraviolet technique showed a rapid increase in absorption upon decreasing the nano size and increasing Aluminium concentration, with a maximum value at 235 nm, corresponding to a photon energy of 5.277 eV, for an Aluminium oxide concentration of 0.9. For the refractive index spectra of the maximum value is (2.134). For a concentration of 0.9, at a wavelength of 300 nm. However, for 0.1 molar concentration, it is equal to 1.031, indicating a decrease in refractive index upon decreasing molar concentration and increasing the nano size. The value of the energy gap decreased from (3.505) eV to (3.376) eV as Aluminum concentration increased, which is associated with a decrease in nano size. The X-ray diffraction findings showed that the unit cells are Hexagonal. It indicates an increase in the density of samples when decreasing the nano size and increasing the molar concentration of aluminium at a rate of 0.8572 mg. The d- spacing decreases when the nano size decreases while the Aluminium concentration increases at a rate of 0.28085×10^{10} m / mole.

Keywords: **Klein-Gordon equation, Maxwell's equations, resonance, friction, free radicals**

.

1. Introduction

The optical properties of materials describe their interactions with electromagnetic radiation. This spectrum includes X-rays, ultraviolet (UV), visible light, infrared, and radio waves. Key optical properties include energy gaps, absorption coefficient, reflection, transmission, and absorbance. [1,2]. Photons may give their energy to the material (absorption); photons may give their energy, but photons of identical energy can be immediately emitted by the material (reflection); photons may not interact with the material structure (transmission). During transmission, photons may change their velocities (refraction). At any instance of light interaction with a material, the total intensity of the incident light striking a surface is equal to sum of the absorbed, reflected, and transmitted intensities [3]. These optical properties can be changed when the atomic and energy structures were changed. Such changes cause limited changes in the optical properties of bulk matter. But recently, new materials known as nanomaterials were found to provide scientists with high flexibility to change optical properties upon changing the atomic structure. Nanomaterials consist of a very large number of isolated particles with dimensions ranging from 1 to 300 nanometers. The behaviour of such nanomaterials obeys quantum laws. The physical properties of nanomaterials can change with changes in the geometry, size, and shape of nanoparticles, nanotubes, or nanosurfaces [4]. Carbon nanotube (CNT), was discovered by SumioIijima in 1991, in the soot of an arc discharge apparatus. The discovery of CNT ignited research on growth, characterization and applications. Development

has exploded due to the amazing electronic and extraordinary mechanical properties of CNT. Thus, CNT can be metallic or semiconducting, and hence provides the potential to create semiconductor-to-semiconductor and semiconductor-to-metal junctions, useful in electronic devices. [5]. Aluminium oxide on the physical attributes of cementitious mortar. [6] The Al_2O_3 nanoparticles (NPs) exist in corundum form that has different phases like γ, β, θ, and δ, the α alumina phase (Al2O3) is the most stable and distinguished thermodynamically and has characteristic properties such as high stability, high hardness, high insulation, and transparency [7]. The absorption of UV/visible radiation occurs by exciting electrons within the molecular structure to a higher energy state [8]. Spectroscopy in the ultraviolet (UV), visible (Vis) and near-infrared (NIR) region of the electromagnetic spectrum is often called electronic spectroscopy because electrons are transferred from low-energy to high-energy atomic or molecular orbitals when the material is irradiated with light [9].

Various attempts were made to study the effects of doping carbon nanotubes and other carbon materials with metals and other elements. One of them is the work done by C. S Chen [10], which is concerned with multi-walled carbon nanotubes (MWNTs)/attempts Cu-doped ZnO composite powders prepared by the co-precipitation method. The findings indicate that the MWNTs can be modified by Cu-doped ZnO nanoparticles with a hexagonal wurtzite structure after annealing at 450 C, with a nanoparticle size of about 15 nm. Two ultraviolet (UV) peaks and a green band centred at about 510 nm are observed in the fluorescence spectrum of the MWNTs/Cu-doped ZnO composite powder annealed at 450 °C. MWNTs and Cu doping significantly improve the UV absorption of ZnO. In the work by Simona [11], nanocomposites composed of aluminium-doped zinc oxide nanoparticles (AZO-NPs) and multiwalled carbon nanotubes (CNTs) were found to act as UV light sensors. of operating at low voltage. Nanocomposite layers were prepared with different AZO-CNT weight ratios. Exposing samples to UV causes a sudden increase in current that decreases when the light is switched off. This indicates narrowing of the energy gap due to the doping process. The work of J. Ceram et. al [12] is also concerned with doping of carbon nanotubes. In their work, Al-doped ZnO thin films were incorporated into multiwalled carbon nanotubes (MWCNTs). The MWCNT ratio ranges from 0.01 to 1.0 w%. The results obtained indicate that the resistance decreases upon increasing MWCNT concentration. The transmittance decreases, and the absorption increases upon increasing MWCNT concentration. The decrease in resistance associated with the increase in absorption is quite natural, as the increase in absorption increases the number of charge carriers. This may be related to a decrease in the band gap. The research by Mohammed Hassan [13] studied the effect of doping multiwalled carbon nanotubes (MWCNTs) with gold (Au) nanoparticles; p-type MWCNTs cause a lowering of the Fermi level, associated with a decrease in the bandgap and an increase in electrical conductivity. Similarly, the work by Mozdolifa [14] indicates that the optical and electrical properties of iron-doped carbon nanotubes changed with varying iron oxide concentration. All these experimental studies indicate that doping carbon nanotubes with metals improves their optical and electrical properties. This motivated to do this work to dope carbon nanotubes with Aluminum oxide. Materials and methods are presented in Section 2. Section 3 is devoted to results and discussion, while Section 4 is concerned with the conclusion.

2. Materials and Method

In this study, graphite was used to form CNT potassium chlorate (K Cl O3), nitric acid (HNO3) and sulfuric acids (H2 SO4) were used. First, 5.0g of graphite (99.995+% purity, 45Im, Aldrich) was slowly added to a mixture of fuming nitric acid (25mℓ) and sulfuric acid (50mℓ). The mixture was kept for 30 minutes. The mixture was cooled down to 5°C in an ice bath. Also 25.0g of potassium chlorate was slowly added to the solution while stirring for 30 minutes. Since a lot of heat was produced while adding potassium chlorate into the mixture, special care during this step is needed to smear out temperature effect. The solution was heated up to 70°C for 24 hours and was then placed in air for 3 days. Most of the graphite precipitated at the bottom, but some reacted carbon was floating. The floating carbon materials were transferred into DI water (1ℓ). After stirring it for 1 hour, the solution was immediately filtrated and the sample was dried. The formed CNT was doped with aluminium oxide at (0.1, 0.3, 0.5, 0.7 and 0.9) Molar. Then the annealed sample was grinded to get the powdered nanoparticles. The crystal structure of all samples characterized at room temperature using a Philips PW1700 X-ray diffractometer (operated at 40 kV and current of 30 mA). The infrared spectra of synthesized FTIR (Fourier Transform Infrared Spectrophotometer) in the range of 400 to 4000 which used to locate the band positions which are given for all samples. The optical properties of all samples were characterized at room temperature using a 1240 UV spectrometer. From the optical spectra of the synthesized samples, calculate all optical properties (Absorption Coefficient, Extinction coefficient, Optical Energy Band Gap, Refractive Index, Real Dielectric Constant and Imaginary Dielectric Constant)

2.1 Characterization Techniques

The Materials Characterization Lab has a wide variety of characterization techniques in the areas of X-ray diffractometer, FTIR (Fourier Transform Infrared Spectrophotometer), and min 1240 UV- Spectroscopy techniques which help to increase the different degrees of understanding why different materials show different properties and behaviors. To investigate the optical properties of CNT (Carbon Nano Tube) was doped by Aluminum oxide by read (0.1, 0.3, 0.5, 0.7 and 0.9) Molar nanoparticles, some precise techniques have been used in our stud. The following characterizations have been potentially performed for the analytical of the synthesized samples.

2.2 Fourier transport infrared spectroscopy (FTIR)

Infrared (IR) spectroscopy is a one-photon effect, and photon absorption results in vibrational motion of a molecule. Infrared spectra originate from the vibrational motions of atoms in chemical bonds within the molecular structure. When a beam of light containing the (IR) radiation interacts with a sample [11]**.** Fourier spectroscopy" is a general term that describes the analysis of any varying signal into its constituent frequency components, Fourier Transform Infrared Spectroscopy (FTIR) is a reliable method of infrared spectroscopy and offers several analytical opportunities in academic, analytical and forensic labs, FT-IR spectroscopy includes the absorption, reflection, emission, or photo acoustic spectrum obtained by Fourier transform of an optical interfere program [12] . The infrared region (10-14000 cm^{-1}) of the electromagnetic spectrum is divided into three regions: the near-, mid-, and far-IR. The mid-IR (400-4000 cm^{-1}) is the most commonly used region for analysis as all molecules possess characteristic absorbance frequencies and primary molecular vibrations in this range. Mid-infrared spectroscopy. Methods are based on the study of the interaction of infrared radiation with samples. As IR radiation is passed through a sample, specific wavelengths are absorbed, causing the chemical bonds in the material to undergo vibrations such as stretching, contracting, and bending. Functional groups present in a molecule tend to absorb IR radiation at the same wavenumber range regardless of other structures in the molecule, and spectral peaks arise from the absorption of vibrational energy changes in the IR region. Thus, there is a correlation between IR band positions and molecular structure. In addition to providing qualitative information about functional groups, IR spectra can yield quantitative information, such as bacterial concentration in a growth medium. An IR spectrum is measured by calculating the intensity of the IR radiation before and after it passes through a sample, and the spectrum is traditionally plotted with the Y-axis in absorbance or transmittance units and the X-axis in wavenumber units. For quantitative purposes, it is necessary to plot the spectrum in absorbance units.

FT-IR absorbance spectra follow Beer 's law, which relates concentration to absorbance as in Eq. (1)

$$A\lambda = L\,\varepsilon\lambda C \qquad (1)$$

Where Aλ_ = Absorbance, L = Path length, ελ = Absorptivity, c = Concentration

Transmittance is not directly proportional to the concentration and is defined in Eq. (2)

$$\%T = \frac{IS}{IR} \qquad (2)$$

Where IS = Intensity of the IR beam after passing through the sample, IR = Intensity of the IR beam before passing through the sample, T = transmittance

Fourier transform infrared (FTIR) spectra of samples were detected using a Mattson Model 960m0016 spectrometer with transmission from 4000 to 400cm^{-1}, using KBr pellets (see Fig. 1).

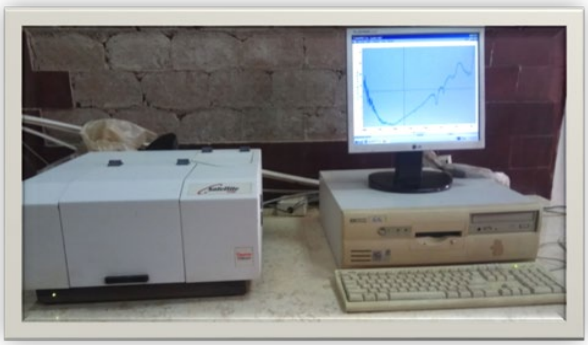

Fig. 1 FTIR (Mattson, model 960m 0016) spectroscopy.

2.3 Ultraviolet -visible spectroscopy (UV-Vis)

Ultraviolet and Visible Spectroscopy is absorption spectroscopy uses electromagnetic radiations between 190 nm to 800 nm and is divided into the ultraviolet (UV, 190-400 nm) and visible (VIS, 400-800 nm) regions. Since the absorption of ultraviolet or visible radiation by a molecule leads transition among electronic energy levels of the molecule, it is also often called as electronic spectroscopy. When radiation interacts with matter, a number of processes can occur, including reflection, scattering, absorbance, Fluorescence/phosphorescence (absorption and reemission), and photochemical reaction (absorbance and bond breaking). In general, when measuring UV-visible spectra, we want only absorbance to occur. Because light is a form of energy, absorption of light by matter causes the energy content of the molecules (or atoms) to increase. The total potential energy of a molecule generally is represented as the sum of its electronic, vibrational, and rotational energies [13]. The absorption spectra of prepared nanoparticles were measured using shimadzu spectrophotometer (UV mini 1240) in 190-800nm range see Figure (2)

Fig. 2 UV mini 1240 spectrometer Shimadzu

2.4 X-ray Powder Diffraction (XRD):

X-ray diffractometers consist of three basic elements: an X-ray tube, a sample holder, and an X-ray detector. X-rays are generated in a cathode ray tube by heating a filament to produce electrons, accelerating them toward a target with an applied voltage, and bombarding the target material with them. When electrons have sufficient energy to dislodge inner shell electrons of the target material, characteristic X-ray spectra are produced. These spectra consist of several components, the most

common of which are Kα and Kβ. Kα consists, in part, of Kα1 and Kα2. Kα1 has a slightly shorter wavelength and twice the intensity as Kα2. The specific wavelengths are characteristic of the target material (Cu, Fe, Mo, and Cr). Filtering, by foils or crystal monochromators, is required to produce monochromatic X-rays needed for diffraction. Kα1and Kα2 are sufficiently close in wavelength such that a weighted average of the two is used. Copper is the most common target material for single-crystal diffraction, with Cu Kα radiation = 1.5418Å. These X-rays are collimated and directed onto the sample. As the sample and detector are rotated, the intensity of the reflected X-rays is recorded. When the geometry of the incident X-rays impinging on the sample satisfies the Bragg Equation, constructive interference occurs, and a peak in intensity occurs. A detector records and processes the X-ray signal, converting it to a count rate, which is then output to a device such as a printer or computer monitor. The geometry of an X-ray diffractometer is such that the sample rotates in the path of the collimated X-ray beam at an angle θ, while the X-ray detector, mounted on an arm, collects the diffracted X-rays and rotates at an angle of 2θ. The instrument used to maintain the angle and rotate the sample is termed a goniometer. For typical powder patterns, data is collected at 2θ from ~5° to 70°, angles that are preset in the X-ray scan**.**

Fig. 3 X-ray diffractometer: XRD (wavelength 1.54 A°)

3. Results and Discussion:

3.1 Optical Results of Carbon-doped Aluminium Oxide samples

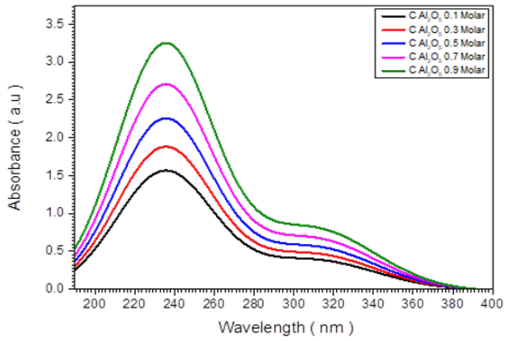

Fig. 4 Relation between absorbance and wavelengths of five carbon-doped aluminium oxide samples having molar concentrations (0.1, 0.3, 0.5, 0.7 and 0.9)

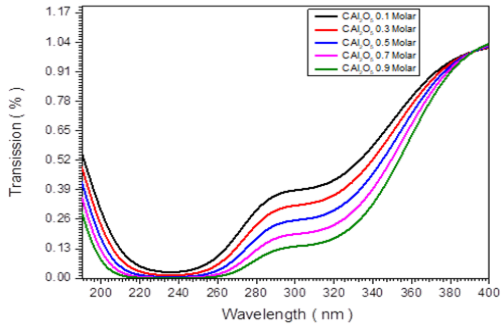

Fig. 5 Relation between transmission and wavelengths of five carbon-doped aluminium oxide samples rated (0.1, 0.3, 0.5, 0.7, and 0.9) Molar

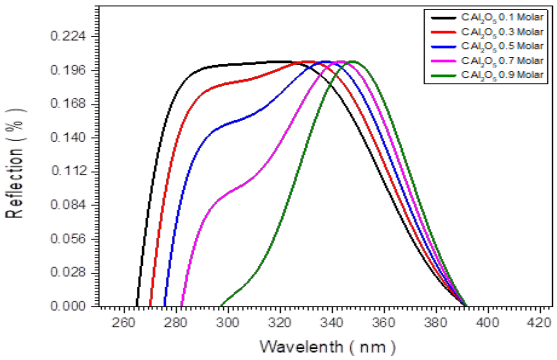

Fig. 6 Relation between reflection and wavelengths of five samples of carbon doped with aluminium oxide having molar concentrations (0.1, 0.3, 0.5, 0.7, and 0.9)

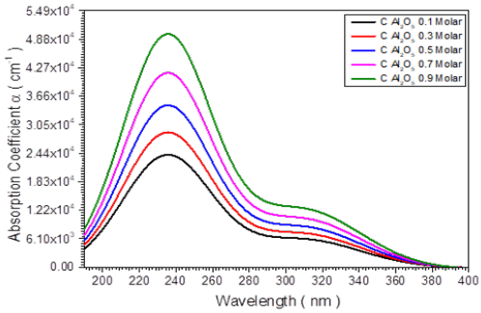

Fig. 7 Relation between absorption coefficient and wavelengths of five Carbon samples doped with aluminium oxide samples having molar concentrations (0.1,0.3,0.5,0.7 and 0.9)

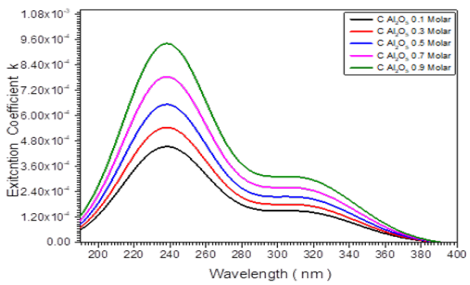

Fig. 8 Relation between extinction coefficient and wavelengths of five Carbon samples doped with aluminium oxide having concentrations (0.1, 0.3, 0.5,

0.7 and 0.9)

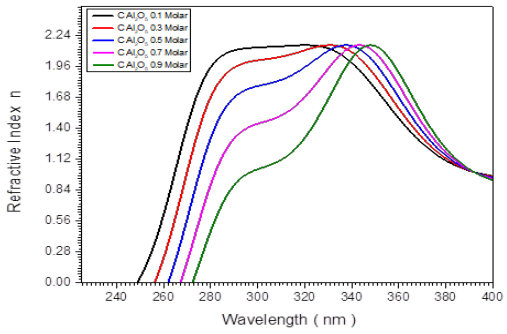

Fig. 9 Relation between refractive index and wavelengths of Carbon samples doped with aluminium oxide samples having molar concentrations (0.1,0.3,0.5,0.7 and 0.9)

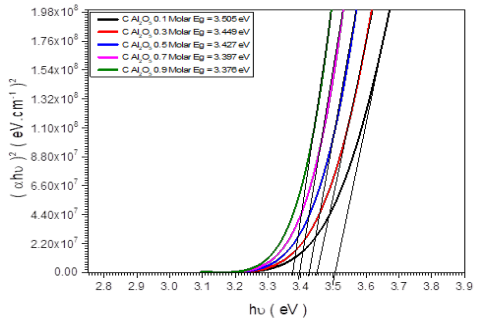

Fig. 10 Optical energy band gap of five Carbon samples doped with aluminium oxide samples having molar concentrations (0.1, 0.3, 0.5, 0.7, and 0.9) Molar

3.2 Results: XRD of Carbon doped with Aluminium Oxide samples

Table 1: Calculated Lattice Constants from Peak Locations and Miller Indices [Hexagonal – primitive] of Carbon doped with Aluminium Oxide 0.9 Molar sample

2Ɵ	d (nm)	h k l
20.856	4.2558	1 1 1
26.641	3.3432	1 0 4

Average Lattice Constants = 8.88943, a = b = 10.029 c = 14.535, α = β = 90^{O} γ = 120^{O} , Density = 6.8301 mg.cm^{-3} , Crystal Form: Hexagonal – primitive, Space Group: R-3c (167) (hexagonal)

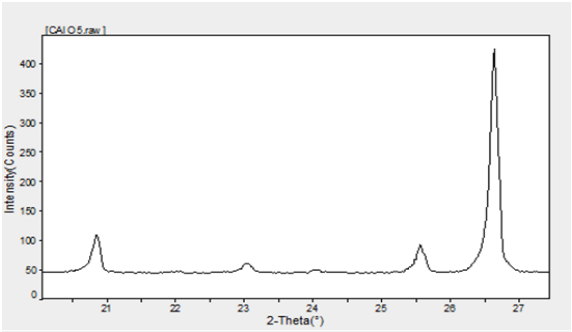

Fig. 11 XRD spectrum of Carbon doped with aluminium oxide at 0.9 Molar concentration

Table 2: Calculated lattice constants from Peak Locations and Miller Indices [Hexagonal – primitive] of carbon doped with aluminium oxide 0.7 Molar sample

2Θ	d (nm)	h k l	Xs(nm)
20.856	4.1458	1 1 1	78.5
26.641	3.2332	1 0 4	67.6

Average Lattice Constants = 8.88943, a = b = 10.029 c = 14.535, α = β = 90^{O} γ = 120^{O} , Density = 6.7344 mg.cm^{-3}, Crystal Form: Hexagonal – primitive, Space Group: R-3c (167) (hexagonal)

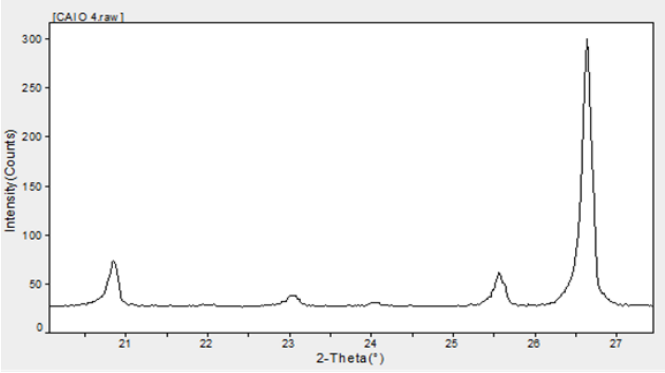

Fig. 12 XRD spectrum of Carbon doped with aluminium oxide at 0.7 Molar concentration

Table 3: Calculated lattice constants from Peak Locations and Miller Indices [Hexagonal – primitive] of carbon doped with aluminium oxide 0.5 Molar sample

2Ɵ	d (nm)	h k l	Xs(nm)
20.856	4.1358	1 1 1	83.7
26.641	3.2232	1 0 4	71.6

Average Lattice Constants = 8.88943, a = b = 10.029 c = 14.535, α = β = 90^{O} γ = 120^{O}, Density = 6.5432 mg.cm^{-3} , Crystal Form: Hexagonal – primitive, Space Group: R-3c (167) (hexagonal).

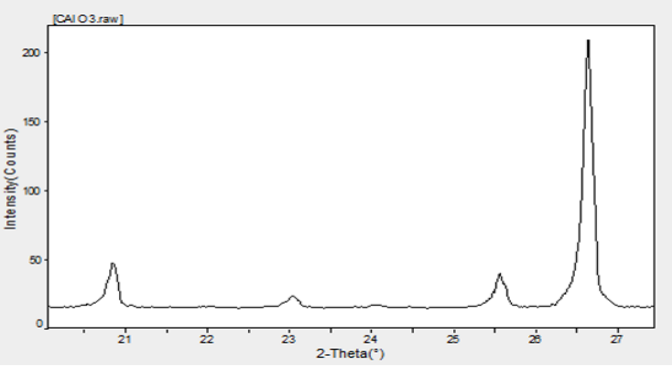

Fig. 13 XRD spectrum of Carbon doping with aluminium oxide 0.5 Molar sample.

Table 4: Calculated lattice constants from Peak Locations and Miller Indices [Hexagonal – primitive] of carbon-doped aluminium oxide (0.3 Molar sample)

2Ɵ	d (nm)	h k l	Xs(nm)
20.856	4.1153	1 1 1	88.4
26.641	3.1032	1 0 4	81.8

Average Lattice Constants = 8.88943, a = b = 10.029 c = 14.535 α = β = 90^{O} γ = 120^{O}, Density = 6.4326 mg.cm^{-3} , Crystal Form: Hexagonal – primitive, Space Group: R-3c (167) (hexagonal).

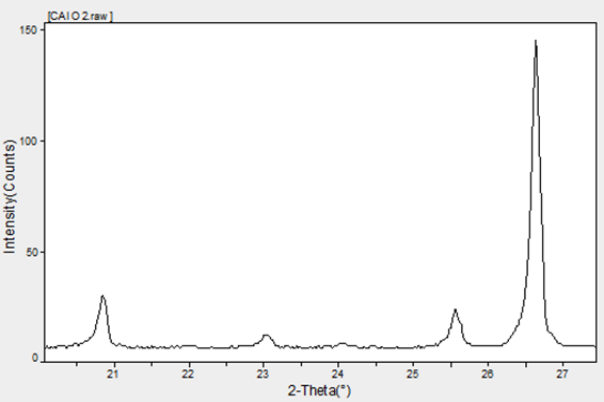

Fig. 14 XRD spectrum of Carbon doping by Aluminum Oxide 0.3 Molar sample

Table 5: Calculated Lattice Constants from Peak Locations and Miller Indices [Hexagonal – primitive] of Carbon doping by Aluminum Oxide 0.1 Molar sample

2Ɵ	d (nm)	h k l	Xs(nm)
20.856	4.2558	1 1 1	103.7
26.641	3.3432	1 0 4	83.6

Average Lattice Constants = 8.88943, a = b = 10.029 c = 14.535, α = β = 90^{O} γ = 120^{O}, Density = 6.1238 mg.cm^{-3} , Crystal Form: Hexagonal – primitive, Space Group: R-3c (167) (hexagonal).

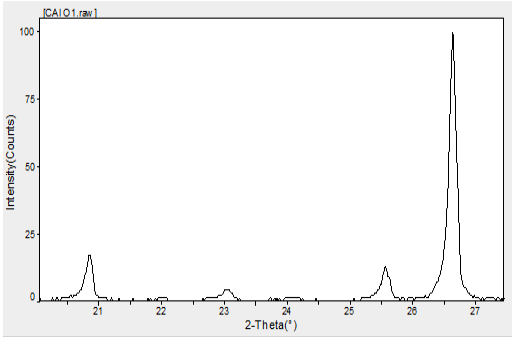

Fig. 15 XRD spectrum of Carbon doping in aluminium oxide 0.1 Molar sample

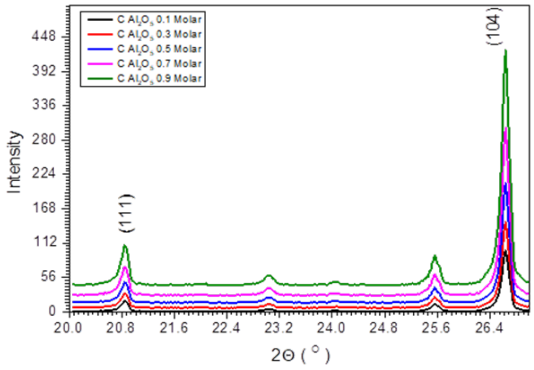

Fig. 16 XRD spectrum of five carbon-doped aluminium oxide samples rated (0.1, 0.3, 0.5, 0.7, and 0.9) Molar

Table 6: some crystallite lattice parameter (c- form, a,b,c, β,α, γ, density, Xs(nm) and d – spacing) of five Carbon doping by Aluminum Oxide samples rated (0.1,0.3,0.5,0.7 and 0.9) Molar

Sample (Carbon doping by Aluminium Oxide)	Density ($mg.cm^{-3}$)	Xs(nm)	d-spacing (10^{10}m)
0.9 M	**6.8301**	**68.65**	**6.60925**
0.7 M	**6.7344**	**73.05**	**6.6795**
0.5 M	**6.5432**	**77.65**	**6.7344**
0.3 M	**6.4326**	**85.1**	**6.7995**
0.1 M	**6.1238**	**93.65**	**6.8301**

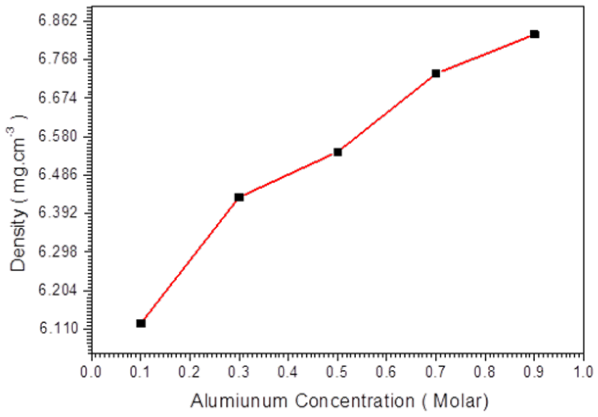

Fig. 17 Relationship between Aluminum Oxide concentration and density of five carbon-doped aluminium oxide samples rated (0.1, 0.3, 0.5, 0.7, and 0.9) Molar

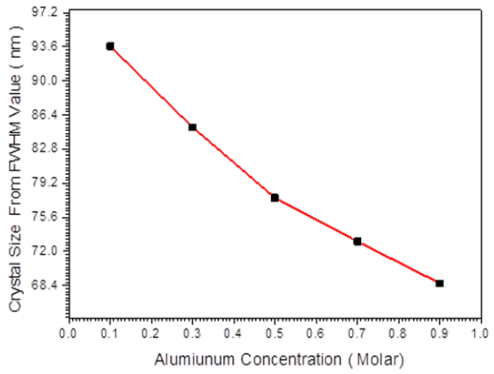

Fig. 18 Relationship between Aluminum Oxide concentration and Crystal Size of five carbon-doped aluminium oxide samples rated (0.1, 0.3, 0.5, 0.7 and 0.9) Molar

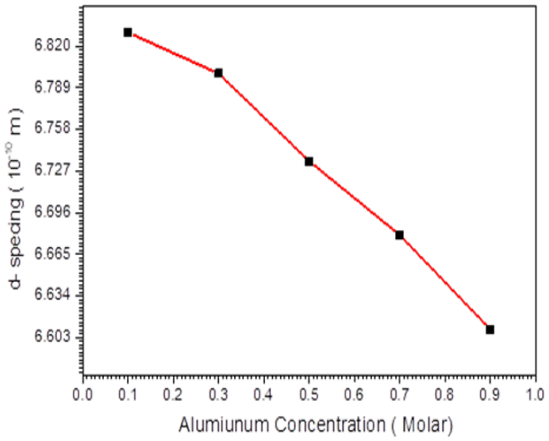

Fig. 19 Relationship between Aluminium Oxide concentration and d-spacing of five carbon-doped aluminium oxide samples rated (0.1, 0.3, 0.5, 0.7 and 0.9) Molar

3.3 Discussion: XRD of Carbon-Doped Aluminium Oxide samples

The crystal structures of all samples are characterized at room temperature about 30 C, using a Philips PW1700 X-ray diffraction meter (XRD) (operated at 40 kV and current of 30 mA) and samples were scanned between 10O and 80O at a scanning speed of 0.06 oC/s using Cu Kα radiation with λ = 1.5418Å. The samples are carbon nanotubes doped with Aluminum Oxide having molar concentrations (0.1, 0.3, 0.5, 0.7 and 0.9) as shown in figs (11) to (19). The unit cells have hexagonal geometry. Tables (1) up to (6) show the XRD parameters, including the crystal nano size and the d-spacing. Fig (17) describes the relation between the molar concentration of aluminium oxide and the density of all samples. The findings showed an increase in sample density with increasing molar concentration of Aluminium Oxide, at a rate of 0.8572 mg. Cm-3/molar. The dislocation density (δ) and number of unit cells (n) are listed in Table (6). Dislocation density decreases as the number of unit cells increases. Fig. 18 shows that increasing aluminium oxide concentration decreases the crystal size at a rate of 31.025 nm/molar. Finally, Fig. 19 shows that decreasing Aluminium oxide concentration increases the d-spacing at a

nearly constant rate of 0.28085 × 10^-10 m/mol.

4 . Conclusion:

The results of doping carbon nanotubes with Aluminium oxide showed that increasing Aluminium oxide concentration increases the density and absorption coefficient. However, the nano size, d-spacing, and energy gap increase as the Aluminium oxide concentration decreases.

References

[1] Ahmed H. A. Elsammani and Hasabalrasoul G. I. Hamza Determination of the Optical Properties of Cobalt Oxide Using Ultraviolet Visible Spectroscopy, Bima Journal of Science and Technology, Vol. 8(3) Sept, 2024 ISSN: 2536-6041,p 156.
[2] Kailas, S. V. (2003). Materials Science: Optical Properties, Chapter 17, Indian Institute of Science, Bangalore, pp. 16- 20.
[3] Swati S. Kulkarni, Mahendra D. Shirsat (2015) Optical and Structural Properties of Zinc Oxide Nanoparticles p (3).
[4] Ahsan MA, Jabbari V, Imam MA, Castro E, Kim H, Curry ML, Valles-Rosales DJ, Noveron JC (2020) Nano scale nickel metal organic framework decorated over grapheme oxide and carbon nanotubes for water remediation. Sci Total Environ 698:134214. https://doi.org/10.1016/j.scitotenv.2019.134214
[5] Z. Raziah,1 and A. R. Junizah, Carbon Nanotubes: A Review on Structure and Their Interaction with Proteins; volume 2013 |Article ID 676815 , (2013). https://doi.org/10.1155/2013/676815 .p18.
[6] **David G. Watson (2017)** Pharmacetical Analysis**,** Fourth Edition**,** Elsevier Limited. All rights reserved, ISBN: 978-0-7020-6989-5, ISBN: 978-0-7020-7029-7, p88.
[7] **H. Heidarzad Moghaddam, M. A. Lotfollahi-Yaghin, A. Malekia (2021)** Durability and Mechanical Properties of Self-compacting Concretes with Combined Use of Aluminium Oxide Nanoparticles and Glass Fiber, International Journal of Engineering, IJE TRANSACTIONS A: Basics Vol. 34, No. 1, P26.
[8] **Afra M. Baghdadi, Amna A. Saddiq, Abdallah Aissa,Yousif Algama and Nagy Mohamed Khalil,** Structural refinement and antimicrobial activity of aluminum oxide nanoparticles**,** Journal of the Ceramic Society of Japan 130 [3], **(2022).** http://doi.org/10.2109/jcersj2.21140 ,P257.
[9] **Weckhuysen, B. M,** Spectroscopy of transition metal ions on surfaces, Weckhuysen, B. M., Van Der Voort, P., Catana, G., (Eds.), Leuven University Press, **.** (2000). p. 221.
[10] C. S. Chen, X. D. Xie, T. G. Liu, L. W. Lin, J. C. Kuang, X. L. Xie, L. J. Lu, S. Y. Cao, Multi-walled carbon nanotubes supported Cu-doped ZnO nanoparticles and their optical property, J Nanopart Res (2012)14:817, DOI 10.1007/s11051-012-0817-5
[11] Simona Fillice, Stefano Boscarino, Mario Scuderi, Sebania Libertino, Clelia Galatic, AZO Nanoparticles - Decorated CNT's for UV Light Sensing: A Structural, Chemical and Electro-Optical Investigation, Nanomaterials, 2023, 13,215
[12] Fang-Hising Wang, Structural, electrical and optical properties of carbon nanotube-incorporated Al-doped zinc oxide thin films prepared by sol-gel method, Journal of Ceramic Processing Research, 2013, V. 14, no.2, pp. 149- 152
[13] Mohammad Hassan, Ramezan Zadehk, Majid Seifi, Maryam Abdolrahimi, Synthesis and comparative study of optical and electrical properties of Au-doped carbon nanotubes prepared in different reaction media, Chinese Journal of Physics, Volume 56, Issue 2, April 2018, Pages 476-483
[14] **Mozdalifa M. Abd Elrahim. Mubarak. D. Abdallah, and Hasabalrasoul. G . Ismail,** Synthesis of Carbon Nanotubes Doped by Iron Oxide in Different Molarity, Al-Butana Journal of Applied Science (BJAS) Issue (11) June 2021- ISSN: 6616, p 60.